ELSEVIER

Chemical Engineering Journal 116 (2006) 13–18

Chemical Engineering Journal

www.elsevier.com/locate/cej

Hydrogen enrichment of a methane–air mixture by atmospheric pressure plasma for vehicle applications

E. El Ahmar*, C. Met, O. Aubry, A. Khacef, J.M. Cormier

GREMI-Polytech'Orléans, 14 rue d'Issoudun, B.P. 6744, 45067 Orléans, Cedex 2, France

Received 19 July 2005; received in revised form 13 October 2005; accepted 14 October 2005

Abstract

During the last few years, the control of motor vehicles pollution has generated considerable research oriented towards the efficiency and the yield of the combustion techniques. A relatively new technology based on the plasma treatment of inlet gases appears to improve the operating conditions of internal combustion engines. The primary focus of this technique is the transformation of methane–air mixture into hydrogen-rich gas before the admission in the cylinder of the vehicle engine.

This work describes an experimental investigation in CH_4–air mixture using a 20 kHz sliding discharge plasma reactor at atmospheric pressure. After plasma treatment, the major gaseous: H_2, CH_4, CO, CO_2 and H_2O were analyzed and quantified using a micro-gas chromatograph (μGC) and Fourier transform infrared absorption spectrometer (FTIR). Plasma treatment results show H_2 enrichment in the range of 4–10% of the inlet gas mixture.

The next step of this preliminary laboratory study will be the engine test bench.

Keywords: Non-thermal plasma; Combustion; Sliding discharges

1. Introduction

Among the existing pollution sources, motor vehicles are seen as a major contributor to air pollution by nitrogen oxides (NO_x), carbon oxides (CO and CO_2), unburned hydrocarbons (UHC) and fine particles matter (PM). The more and more constraining environmental regulations have motivated investigations for decreasing the fuel consumption and reduce drastically pollutant emissions. These objectives require the improvement of the combustion processes and a better understanding of ignition and combustion chemistry.

Thermal plasmas have been applied to combustion over the past three decades with success, particularly in the conversion of fuel–air mixtures into H_2 and CO in efforts to increase internal combustion engine efficiency and to reduce NO_x emissions [1,2].

Non-equilibrium plasmas created by electrical discharge are potentially useful for promoting combustion. In such plasma, the formation of reactive species eventually accelerates the chemical conversions and the reforming reactions. The result is the production of H_2-rich mixture. A broad range of hydrocarbons can be treated by this way. Plasma treatment may favor partial oxidation by reducing the production of soot. The on-board production of hydrogen could thus favor the ignition of combustion in lean burn engines [1–4]. Hydrogen significantly increases the flame propagation rate flame and enlarges the possibilities of using lean-burn mixtures by avoiding misfiring. This approach seems particularly attractive for gasoline and natural gas engines since a small quantity of hydrogen could enable correct operation in the case of lean-burn mixtures.

The objective of the present work is to evaluate the plasma treatment of air–fuel mixture applied to internal combustion engines. Preliminary results obtained in a laboratory scale reactor operating at conditions close to those of thermal engines are presented. These results show the possibilities to obtain an H_2-rich mixture from CH_4–air mixture.

2. Experimental setup

A sliding discharge reactor operates according to the principle of "Glidarc" discharge previously studied in GREMI laboratory for several types of applications [5–10]. The construction of the reactor was simplified in order to rapidly assess the reactor

* Corresponding author. Tel.: +33 2 38 49 46 00; fax: +33 2 38 41 71 54.
E-mail address: elise.el-ahmar@univ-orleans.fr (E. El Ahmar).

1385-8947/$ – see front matter © 2005 Elsevier B.V. All rights reserved.
doi:10.1016/j.cej.2005.10.005

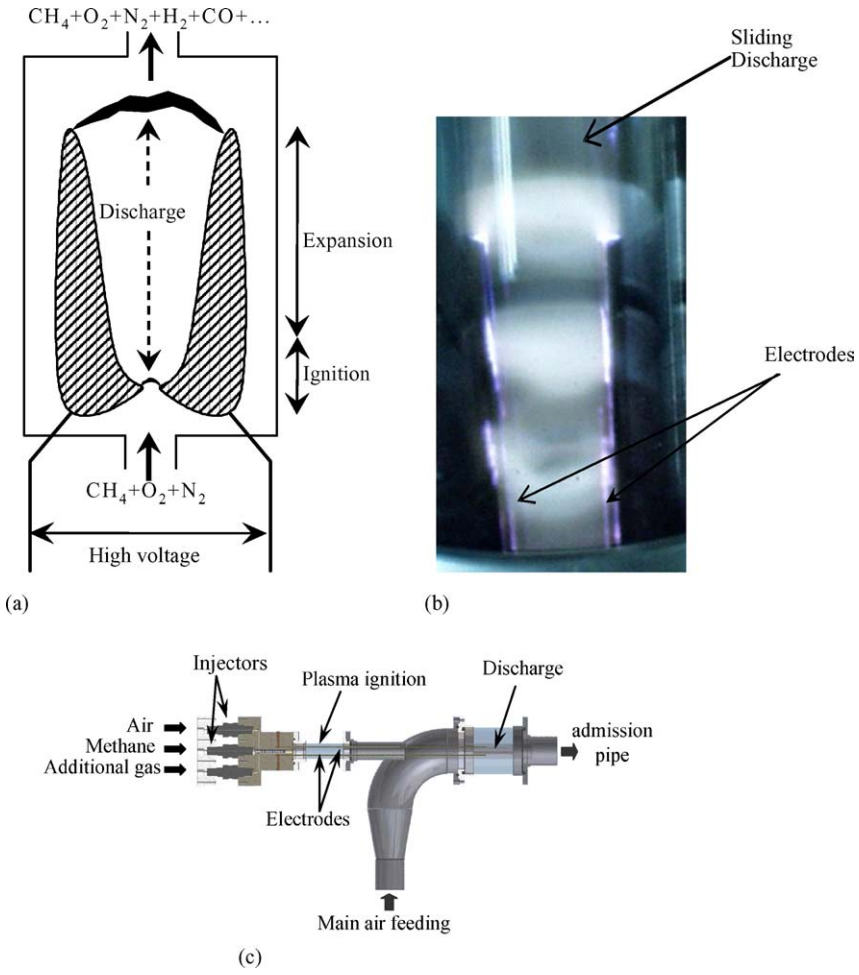

Fig. 1. Experimental reactor. (a) Schematic of sliding discharge, (b) photography of sliding discharge and (c) motor bench reactor.

possibilities for the planned application. The reactor consists of a quartz tube (length, 300 mm; inner diameter, 22 mm) in which two parallel electrodes are laid out. The electrode gap is about 1 mm near the gas mixture injector (ignition; Fig. 1a) in order to ignite the discharge. The plasma column thus created is carried along the electrodes and is elongated at their extremities before being extinguished, giving rise to a new discharge in the ignition space [11–14]. The phenomenon is periodic and the lifetime of a discharge decreases with increasing the gas flow rate.

Fig. 1a and b shows the schematic of the sliding discharge device and photography of the reactor in operation, respectively. Fig. 1c presents a schematic of the test motor bench reactor.

The power supply operating conditions must be flexible in order to allow a synchronization between the discharge and the admission of gases in the engine combustion chamber. According to the engine regime, the plasma treatment duration must be regulated. At a speed of 2000 rounds per minute, this duration is approximately 15 ms. This power supply consists of a symmetric square waveform voltage with a step-up transformer. The discharge is directly connected to the secondary coil of the transformer. Because of leakage fluxes, discharge current waveform is determined by the primary voltage, reactance and resistance of winding.

Voltages and currents were measured with an ST500 probe connected to a voltage divider (ratio, 0.01) and a Hall effect probe Tektronix TCP 202, respectively. The signals from the probes were recorded on a Tektronix TDS 460A digital oscilloscope and processed in a PC.

On Fig. 2, typical voltage and current are plotted with a phase angle of 180° in order to clarify the presentation (real phase angle is 0°). The voltage and current oscillations over the mean waveform are typical of backbreakdown phenomenon [15]. Backbreakdown number is a function of the gas velocity and it is about 13 per cycle in our experiments. The electrical power is calculated from voltage–current recordings and deter-

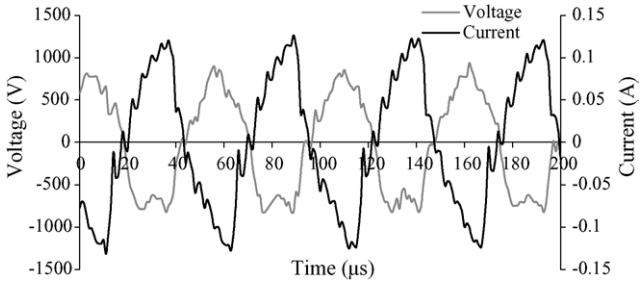

Fig. 2. Current and voltage with CH_4 (19%)–air.

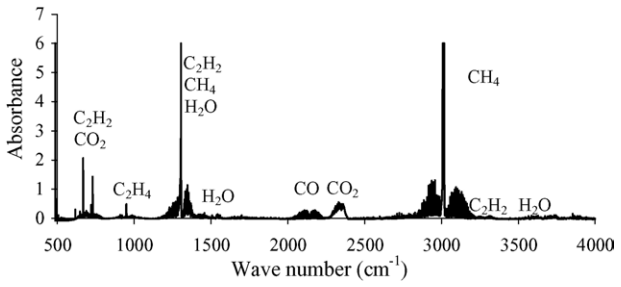

Fig. 3. Typical IR spectrum (CH_4 (19%)–air, electrical power = 50 W).

mined by averaging the instantaneous power over two sliding periods.

The experiments were conducted at atmospheric pressure and room temperature. Air–methane experiments were carried out with methane concentrations higher than the upper explosive limit (15%) [16], i.e. ranging from 16 to 35%. Mixtures with higher CH_4 concentration had been not studied because of carbon deposition phenomena.

After plasma treatment, the output gases were taken over and cooled down in order to eliminate water. Dry output gases (O_2, N_2, H_2, CH_4, CO and CO_2) were analyzed and quantified with Fourier transform infrared spectroscopy (FTIR, Nicolet Magna 550, equipped with a heated 10 m multiple pass absorption cell) and micro gas chromatography (μGC, Varian CP2003P) [16,17]. The H_2O concentration was estimated by considering material balance.

The mean exhaust gas temperature was measured by thermocouples (type K) placed at the outlet of the plasma reactor.

3. Experimental results and discussion

Analyses of formed species were carried out for two series of experimental conditions:

(i) input electrical power varying from 35 to 75 W while CH_4 and air concentrations remain constant;
(ii) CH_4 concentration varying from 16 to 35% while electrical power and air flow rate remain constant.

The major products observed by FTIR spectroscopy were CO, CO_2 and H_2O and the by-products were C_2H_2, C_2H_4 and C_2H_6. A typical IR spectrum is shown in Fig. 3.

3.1. Electrical power effect on CH_4 conversion and H_2 production

Since the device implanted in a thermal engine must be a low energy consumer, we arbitrarily set the electrical power used in these preliminary experiments at several tens of watts (35–75 W).

An example of the mole fractions variation for different species observed after the CH_4 (19%)–air plasma processing as a function of the electrical power are shown in Fig. 4 (symbols). For the maximal power (75 W), CH_4 conversion is about 58% and H_2 production is about 9%. One can note that the changes in CH_4 conversion and H_2 production are not linear since for a power of 35 W, the CH_4 conversion rate is about 13% and H_2 production is 2.5%. The CH_4 conversion and the H_2 production are increasing functions of power supplied to the plasma.

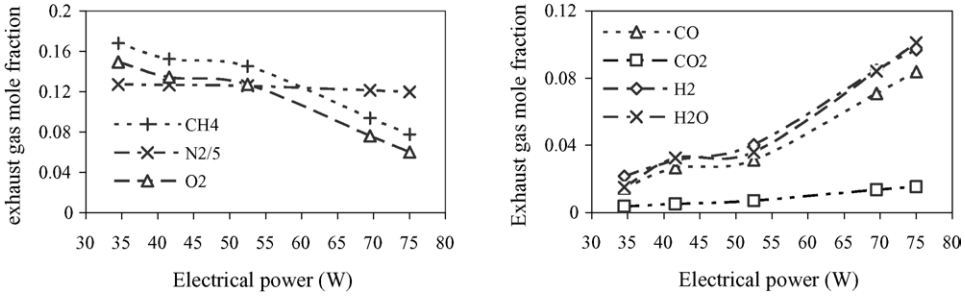

Fig. 4. Experimental (symbols) and adjusted (dashed lines) exhaust gas composition as a function of electrical power (total flow rate = 41 l/min) (CH_4, N_2, O_2, H_2, CO and CO_2 are expressed in dry basis, H_2O is estimated).

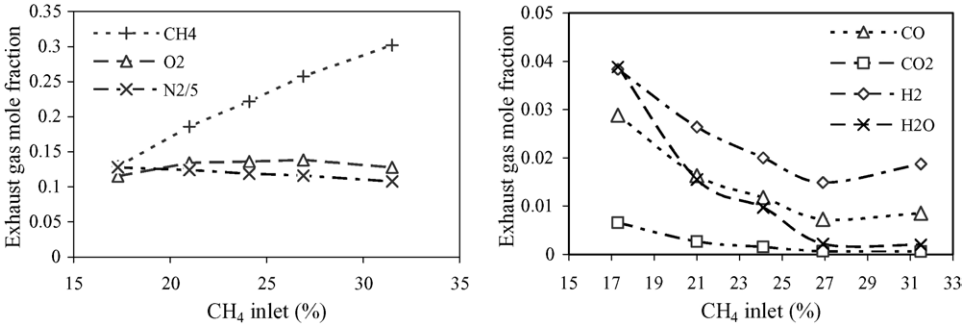

Fig. 5. Experimental (symbols) and adjusted (dashed lines) exhaust gas composition as a function of CH_4 inlet (air flow rate = 33 l/min and electrical power = 50 W) (CH_4, N_2, O_2, H_2, CO and CO_2 are expressed in dry basis, H_2O is estimated).

3.2. Initial CH_4 mole fraction effect on CH_4 conversion and H_2 production

The mole fractions variation for different species observed after CH_4–air plasma processing as a function of initial CH_4 mole fractions are shown in Fig. 5 (symbols). In these experiments the air flow rate and the electrical power were maintained constant at 33 l/min and 50 W, respectively. H_2O, H_2, CO and CO_2 concentrations increase with decreasing the initial CH_4 concentration. H_2O production indicates that a combustion process has been ignited.

4. Three reactions model

The above results show that H_2 enrichment causes a significant CH_4 consumption, a part of which is totally oxidized. The calorific capacity of the combustible mixture is thus considerably modified, explaining the necessity to present an energy balance study in order to discuss the efficiency of the method.

Taking into account the chemical results presented in paragraph 3, a set of three chemical reactions is used to compare the electrical power consumed in the system with the chemical energy exchanged per unit of time.

$$CH_4 + 2O_2 \rightarrow CO_2 + 2H_2O, \quad \Delta H_1 = -802.34\,\text{kJ/mol} \quad (1)$$

$$CH_4 + 1/2O_2 \rightarrow CO + 2H_2, \quad \Delta H_2 = -35.72\,\text{kJ/mol} \quad (2)$$

$$CH_4 + 3/2O_2 \rightarrow CO + 2H_2O, \quad \Delta H_3 = -519.36\,\text{kJ/mol} \quad (3)$$

The change in the composition of the outlet gas mixture can be expressed in terms of progress variables, which represent the proportion of limiting reagent (CH_4) transformed in the reaction. We defined α, β and γ as the progress variables of reactions 1, 2 and 3, respectively. Each chemical species concentration can thus be expressed as a function of α, β and γ.

The α, β and γ coefficients was calculated from the experimental data and the calculated mole fraction using the least square method. The validity of the description using these three coefficients (also called fitting model) is shown by the following results.

4.1. Electrical power effect

Fig. 6 shows the progress variables as a function of the input electrical power. From this data, CH_4 partial oxidation (reaction 2) seems to be the predominant reaction. The coefficients α, β and γ increase with increasing the electrical power. For the lower power used in these experiments (34 W), values of α, β and γ values reach their minima. The validity of the description using progress variables is shown in Fig. 4, where experimental results (symbols) are compared to fitting model (dashed lines).

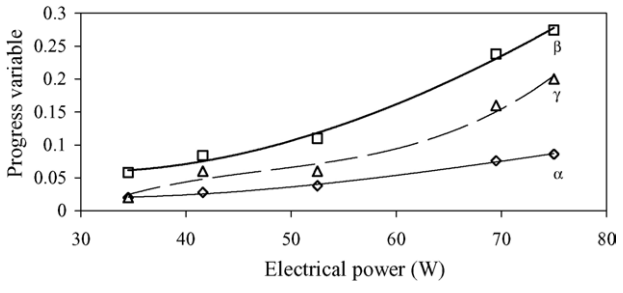

Fig. 6. Progress variables as function of electrical power (total flow rate = 41 l/min).

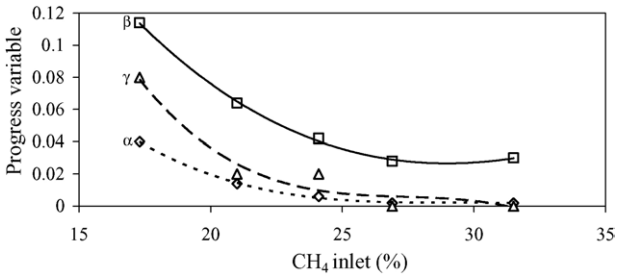

Fig. 7. Progress variables as function of CH_4 inlet (air flow rate = 33 l/min and electrical power = 50 W).

4.2. Initial CH_4 mole fraction effect

Fig. 7 shows the progress variables as a function of the initial CH_4 concentration. As mentioned in the previous paragraph, the data of Fig. 7 shows that CH_4 partial oxidation is the predominant reaction. O_2 consumption increases considerably in the depleted mixtures since the N_2/O_2 ratio increases from 4.2 to 5.5 for the most depleted mixture. Probably an O_2 proportion reacts with CH_4 to form H_2 and CO.

The α and γ values approach zero when CH_4 concentration reaches 30%. The decrease of coefficient β is also significant. These three progress variables reach their maximal values for the minimal CH_4 composition. In that case, the CH_4 consumption is maximal.

The experimental mole fractions of outlet gases were compared to those calculated from the progress variables. Results are given in Fig. 5 (experimental results, symbol; fitting model, dashed lines) and shows that the simplified three chemical reactions correctly describe the process.

5. Absorbed power and physical characterization

5.1. Exhaust gas temperature

The discharge produces a heating of the system. The heating is supplied from two main sources: (i) the electrical energy furnished to the plasma by Joule effect and (ii) the energy supplied by exothermal reactions ignited by the plasma. The exhaust gas temperature was measured using thermocouple placed at 6 cm from the discharge.

Fig. 8 shows the exhaust gas temperature as a function of the initial CH_4 mole fraction. The outlet gas temperature decreases with increasing the initial CH_4 mole fraction. The maximum gas temperature was observed for a CH_4 concentration of about 17%, which corresponds to a strong reactivity of the system. This rise in exhaust gas temperature, which increases when one

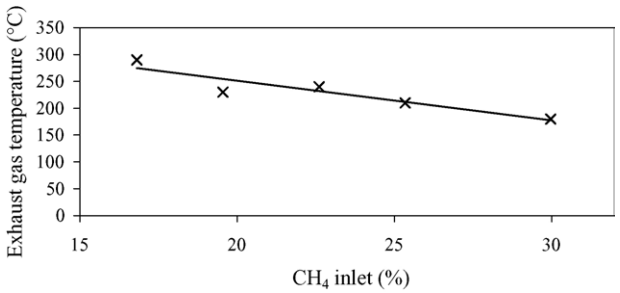

Fig. 8. Outlet reactor gas temperature as a function of CH_4 (air flow rate = 33 l/min and electrical power = 50 W).

approaches the high explosive limit, is probably related to the starting of the combustion process.

5.2. Energy balance

The energy balance of the system is presented by introducing the different power contributions:

(i) P_e, electrical power determined from current–voltage waveforms;

(ii) P_c, power generated by the chemical reactions (in standard conditions) calculated from α, β and γ, as a function of standard enthalpy ΔH^0 (kJ/mol) and CH_4 flow rate D (mol/s);

$$P_c = \Delta H^0 D \quad (4)$$

where the standard enthalpy ΔH is given by:

$$\Delta H^0 = \alpha \Delta H_1 + \beta \Delta H_2^0 + \gamma \Delta H_3 \quad (5)$$

(iii) P_p, power lost by heating products, calculated from α, β and γ, as a function of enthalpy ΔH (kJ/mol) and of the methane flow-rate D (mol/s).

$$\Delta H = \alpha C_{p1} \Delta T + \beta C_{p2} \Delta T + \gamma C_{p3} \Delta T \quad (6)$$

where C_{pi} and ΔT are the calorific capacity of each species and temperature variation between initial and final states, respectively.

$$P_p = \Delta H D \quad (7)$$

P_c and P_p are decreasing functions of the initial CH_4 mole fraction (Fig. 9). By adding P_c and P_e, we obtain the total power furnished to the system (P_t). Taking into account a perfect energy balance, this power (P_t) must correspond to the sum of the heating products power P_p and the power loss in the reactor (P_l). Then, the power loss in the reactor (P_l) is derived from the following relation:

$$P_l = P_e + P_c - P_p \quad (8)$$

Fig. 9 shows that the power generated by the chemical reactions (P_c) is higher than the electrical one (P_e) for CH_4 concentration lower than 23.5%. Also, it is shown that the power losses (P_l) and the one used for heating the products (P_p) have the same order of magnitude.

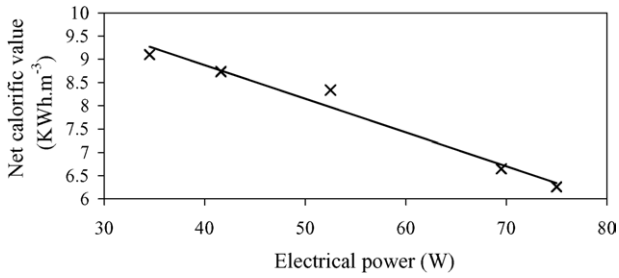

Fig. 10. Net calorific value of CH_4–H_2 mixture as a function of electrical power (total flow rate = 41 l/min).

5.3. Calorific value of the outlet mixture (CH_4–H_2)

The mixture net calorific value (C_m) is calculated from the relation:

$$C_m = \sum (X_i C) \quad (9)$$

where X_i and C are the mole fraction and the net calorific value of each component, respectively.

The net calorific values of H_2 and CH_4 are 2.98 and 9.95 kWh/m^3, respectively. The net calorific value of the outlet CH_4–H_2 mixture was calculated and results are presented as a function of electrical power (Fig. 10). C_m is a decreasing function of the electrical power provided to plasma. Indeed, as previously announced, the CH_4 to H_2 conversion efficiency is as high as the electrical power provided to plasma is high. The weakest C_m value (6.25 kWh/m^3) was obtained for the maximum power (75 W in that study). This result shows that the H_2 enrichment generates fuel mixtures releasing less energy (C_m value) than methane (C value).

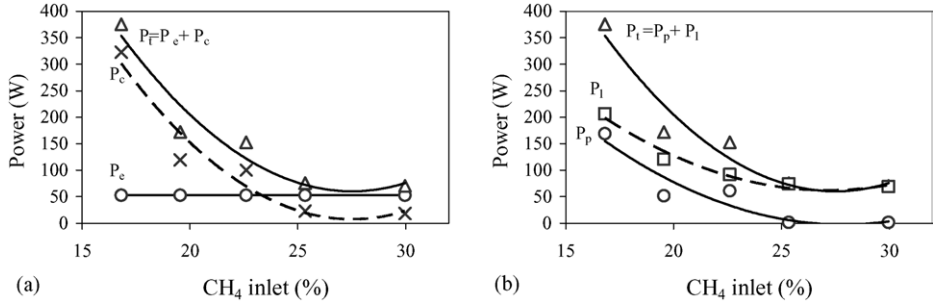

Fig. 9. Various powers as function of CH_4 inlet (air flow rate = 33 l/min and electrical power = 50 W). (a) Total input power and (b) total output power.

6. Conclusion

The treatment of methane–air mixture by plasma at atmospheric pressure, as well as the chemical analysis of the gas products, was carried out. Only, the major products: H_2, CO, CO_2 and H_2O were presented. The hydrogen mole fraction in outlet gas is about 9% for an electric power supplied of 75 W. The reduction of the net calorific value shows that the only interest would be to support the ignition of combustion and the emission reduction.

More work is needed in order to enhance the H_2 concentration produced as well as the energy efficiency. Beside the optimization of the discharge parameters, experiments on the motor bench are envisaged soon.

Acknowledgment

This work was performed within the framework of the French energy program “improvement of the combustion techniques”. The authors are grateful to CNRS and to the Ministère de la recherche for their financial support.

References

[1] L. Bromberg, D.R. Cohn, A. Rabinovich, J.E. Surma, J. Virden, Int. J. Hydrogen Energy 24 (1999) 341–350.
[2] L. Bromberg, D.R. Cohn, A. Rabinovich, J. Heywood, Int. J. Hydrogen Energy 26 (2001) 1115–1121.
[3] R. Breashers, H. Cotrill, J. Rupe, First Symposium on Low Pollution Power Systems Development, Ann Arbor SEMI, 1973.
[4] D.R. Cohn, A. Rabinovich, C.H. Titus, L. Bromberg, Int. J. Hydrogen Energy 22 (1997) 715–723.
[5] F. Richard, J.M. Cormier, S. Pellerin, J. Chapelle, J. Appl. Phys. 79 (1996) 2245–2250.
[6] F. Richard, J.M. Cormier, S. Pellerin, J. Chapelle, J. High Temp. Mater. Process. 2 (1997) 239–248.
[7] F. Richard, J.M. Cormier, S. Pellerin, V. Dalaine, J. Chapelle, Prog. Plasma Process. Mater. (1997) 343–351.
[8] V. Dalaine, J.M. Cormier, P. Lefaucheux, J. Appl. Phys. 83 (1998) 2435–2441.
[9] I. Rusu, J.M. Cormier, Chem. Eng. J. 91 (2003) 23–31.
[10] I. Rusu, J.M. Cormier, Int. J. Hydrogen Energy 28 (2003) 1039–1043.
[11] E. Hnatiuc, V. Dalaine, J.M. Cormier, S. Pellerin, Proceedings of the 6th International Conference on Optimisation of Electrical and Electronic Equipments, OPTIM, 1998.
[12] S. Pellerin, J.M. Cormier, F. Richard, K. Musiol, J. Chapelle, J. Phys. D: Appl. Phys. 32 (1999) 891–897.
[13] S. Pellerin, F. Richard, J. Chapelle, J.M. Cormier, K. Musiol, J. Phys. D: Appl. Phys. 33 (2000) 2407–2419.
[14] A. Kaminska, J.M. Cormier, S. Pellerin, O. Martinie, J. High Temp. Mater. Process. 5 (2001).
[15] S. Pellerin, O. Martinie, J.M. Cormier, J. Chapelle, P. Lefaucheux, J. High Temp. Mater. Process. 3 (2) (2001) 167–180.
[16] C. Met, A. Khacef, J.M. Cormier, Proceedings of the 4th International Symposium of Non-Thermal Plasma Technology for Pollution Control and Sustainable Energy Development, 2004.
[17] C. Met, O. Aubry, A. Khacef, J.M. Cormier, Proceedings of the 9th International Symposium on High Pressure, Low Temperature Plasma Chemistry, 2004.